Appendix - Supplementary Tables and Figures

Table S1. Results of co-registration intercomparison. The table shows glacier-wide mean values ± NMAD (over the glacier, without interpolation of data voids) for two co-registration approaches using two masks of stable terrain.

Co-registration method	Stable terrain mask	Modified stable terrain mask
Berthier and others (2007)	−5.59 ± 3.28	−3.00 ± 3.26
Nuth & Kääb (2011)	−4.68 ± 3.33	−3.86 ± 3.34

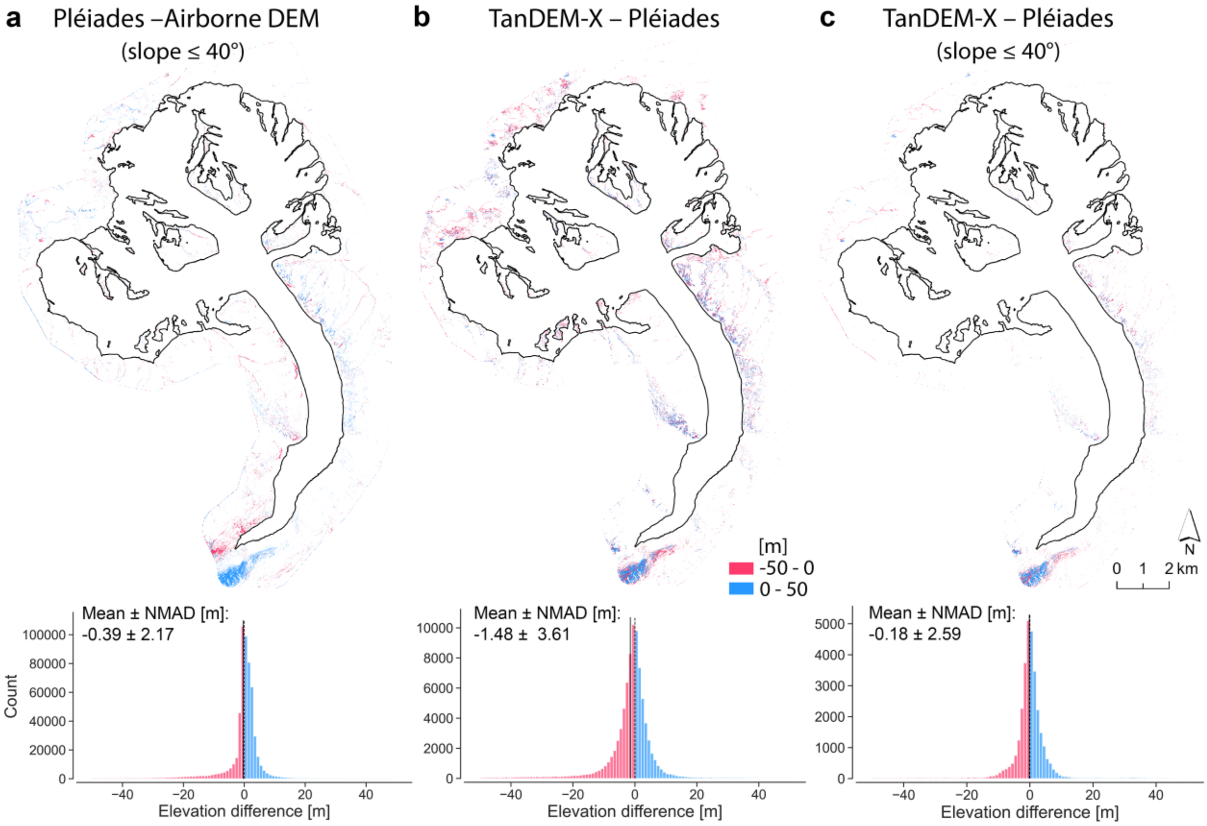

Fig. S1. Elevation difference maps after co-registration on the stable terrain mask and the corresponding frequency distribution coloured by positive (blue) and negative (red) values. Error statistics were calculated on the stable terrain mask excluding slopes above 40°. Elevation differences larger than ±50 m after the co-registration were removed (see section 2.6). (a) Elevation difference map between Pléiades and airborne DEM on common stable terrain pixels (snow free, less than 40°, approx. 2.24 km^2). (b) Elevation difference map between TanDEM-X DEM and Pléiades DEM on common stable terrain pixels (snow free, including steep areas used for co-registration). (c) Same elevation differences as in panel (b) but excluding pixels in steep areas (>40°, approx. 1.12 km^2) used to calculate the error statistics of the glacier elevation differences between TanDEM-X DEM and Pléiades (Table 2). Note that the blue and red patches south of the glacier tongue are caused by different elevations derived by TanDEM-X and Pléiades over single trees and sparse forest of different heights (Praaks and others 2012, Piermattei and others 2019). Also, note that the total pixel count between the co-registration methods differs due to different techniques to shift, resample, and filter the results in combination with abundant data voids.

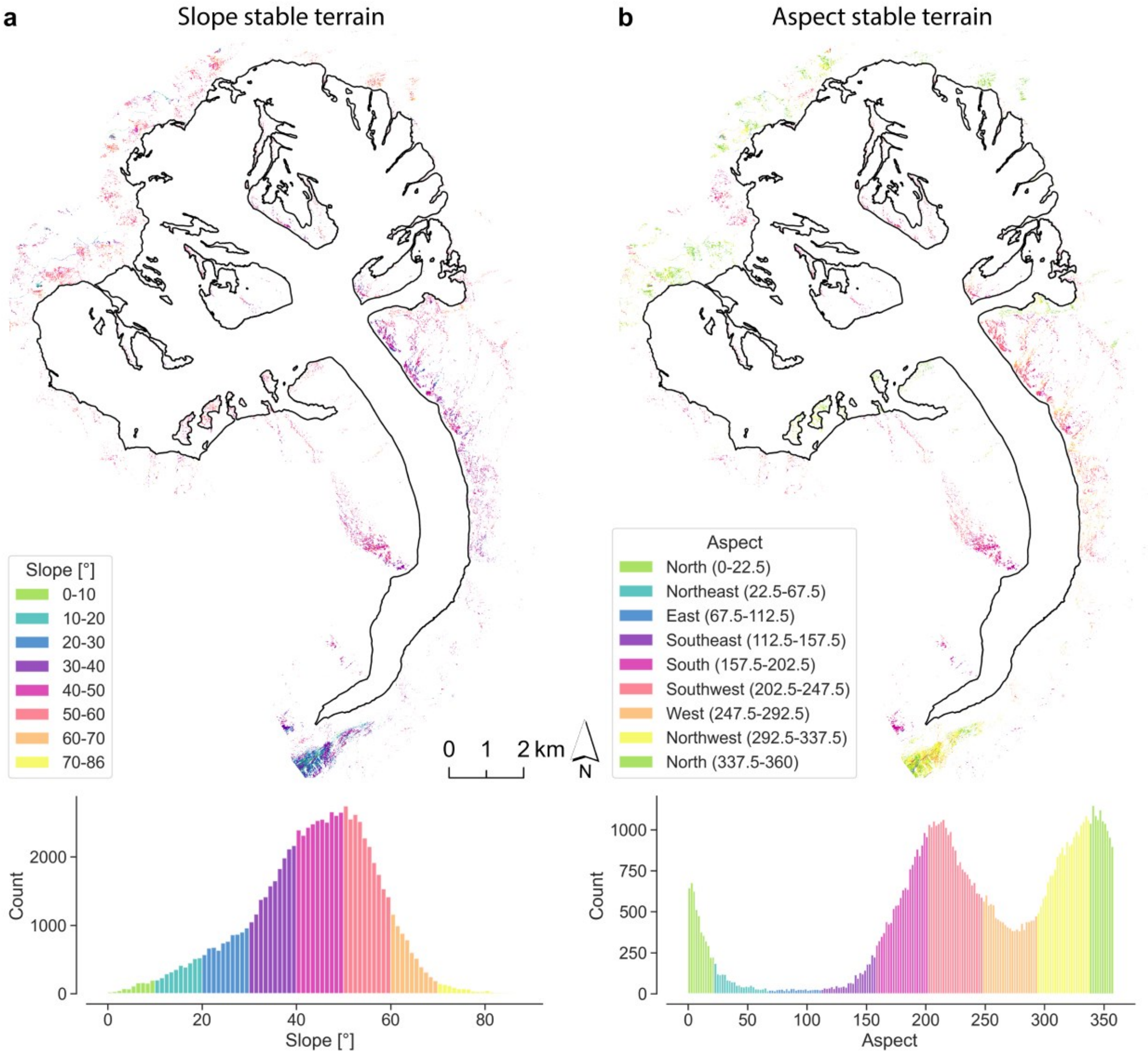

Fig. S2. Distribution of slope (a) and aspect (b) of stable terrain areas used for the co-registrations between Pléiades and TanDEM-X. The maps show that the off-glacier terrain is well distributed around the glacier and does show a good coverage of slope and aspect, required for co-registration.

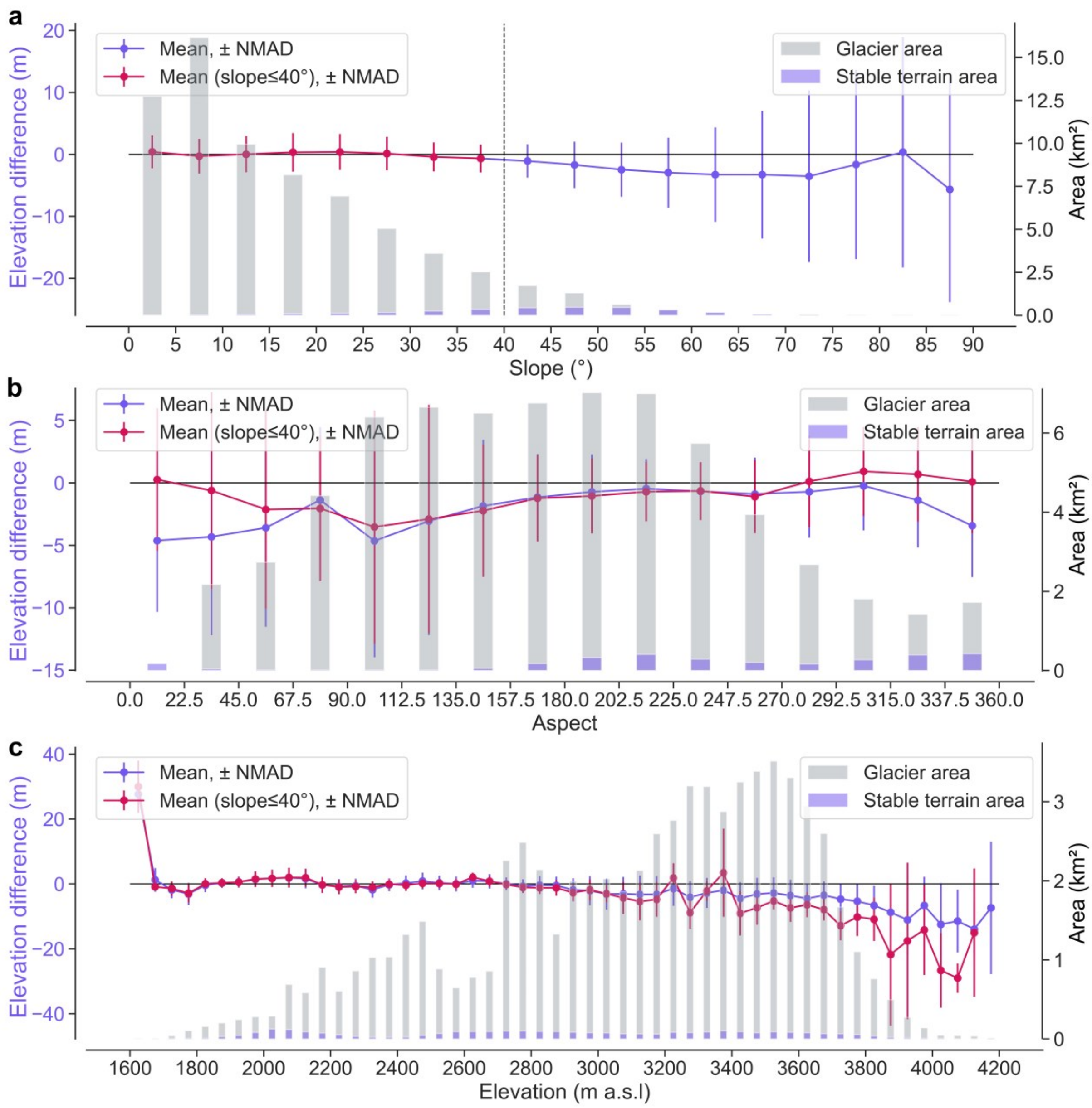

Fig. S3. Elevation differences over stable terrain with respect to slope (a), aspect (b), and elevation (c). Corresponding distributions for glacier and stable terrain areas are given on the second y-axis. Elevation differences are calculated from TanDEM-X minus Pléiades DEMs. Slope, aspect, and elevations are derived from the Pléiades DEM. Note that the graphs based on pixels with slopes ≤ 40° would better represent the elevation differences over the glacier but are subject to insufficient sample size in many elevation bins.

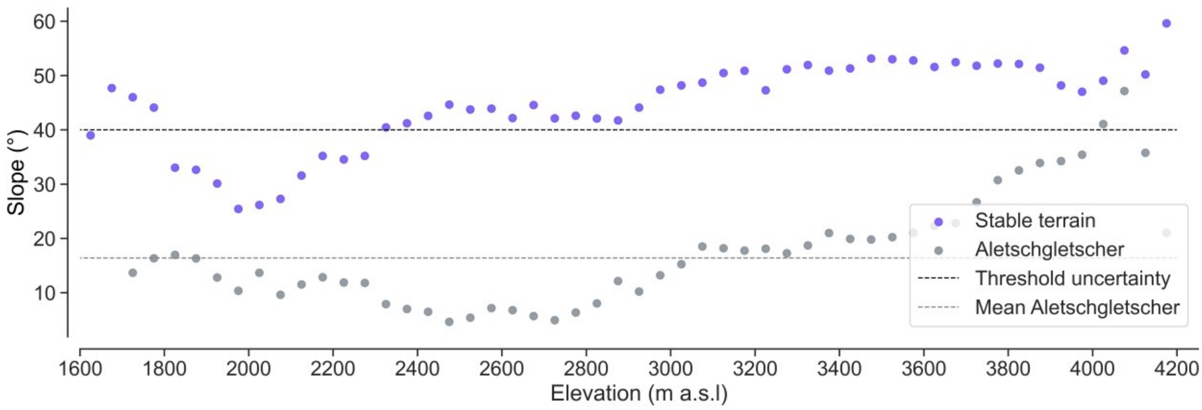

Fig. S4. Slope distribution with elevation over the glacier and over the stable terrain. The black dashed line indicates the slope threshold used in the uncertainty assessment (Section 2.6); the grey dashed line indicates the mean slope over the glacier. Slope and elevation are derived from Pléiades DEM.

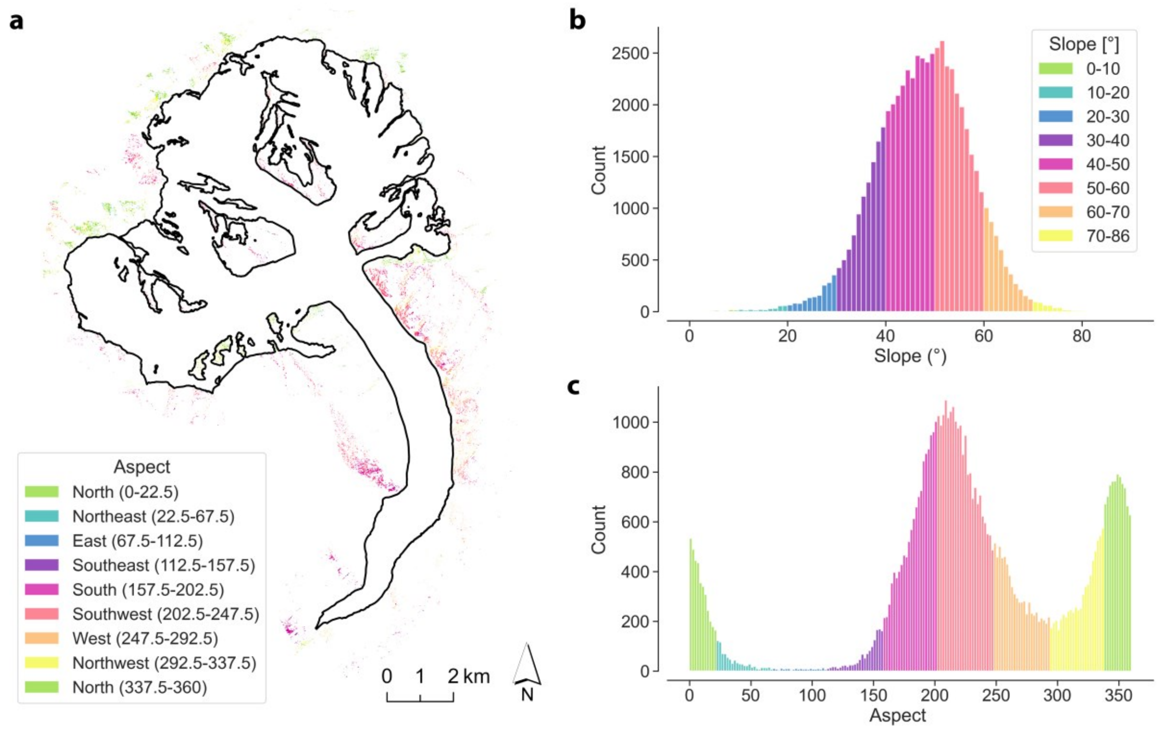

Fig. S5. Distribution of aspect (a, c) and slope (b) of modified stable terrain areas used for the co-registration intercomparison experiment between Pléiades and TanDEM-X. The map and histograms show the off-glacier terrain as in **Fig. S2** but after removal of pixels of lower confidence due to their location in sparse forest and dark shadow areas. Note the strongly reduced count of pixels for slopes ≤40° in the modified mask of stable terrain (**Fig. S2**).

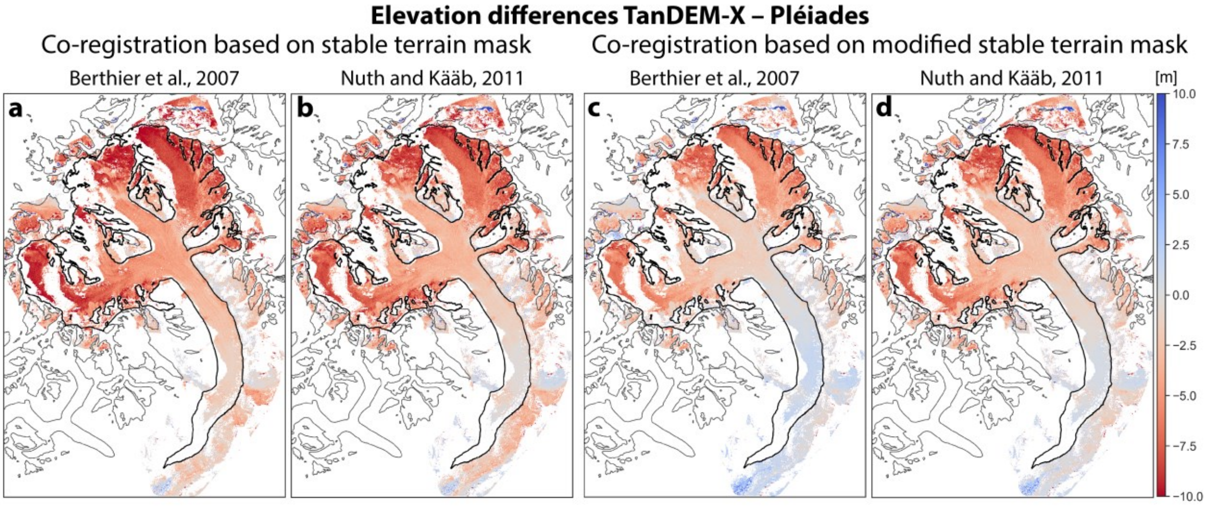

Fig. S6. Elevation difference maps for the co-registration inter-comparison. The elevation differences (TanDEM-X minus Pléiades) for the co-registration by Berthier and others (2007) using the stable terrain mask – as applied throughout the paper – are shown in subplot (a), and using the modified stable terrain mask **(Fig. S5)** in subplot (c). The results for co-registration by Nuth and Kääb (2011) using the stable terrain mask and the modified stable terrain mask are shown in subplots (b) and (d), respectively.

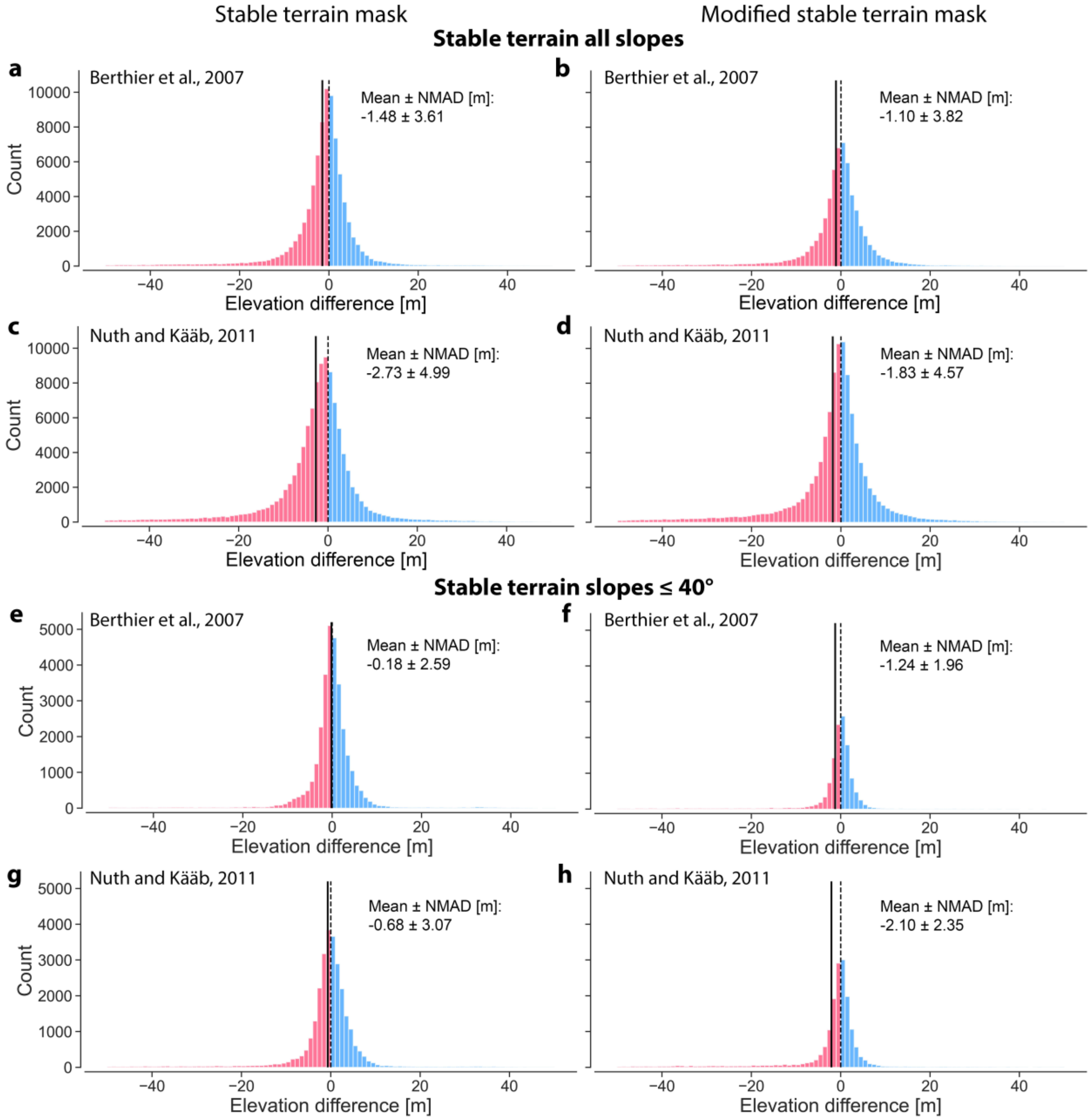

Fig. S7. Stable terrain statistics for the co-registration inter-comparison. The results for the co-registration by Berthier and others (2007) are shown in subplots (a, b, e, f) and by Nuth and Kääb (2011) in subplots (c, d, g, h). Throughout the paper, the co-registration by Berthier and others (2007) using the stable terrain mask is used (a), and statistics for stable terrain ≤40° are considered most representative of elevation differences over the glacier (e; **Table 2**). Note that elevation differences outside the range ±50 m were removed after co-registration. Also, note that the total pixel count between the co-registration methods differs due to different techniques used to shift, resample, and filter the results in combination with abundant data voids.

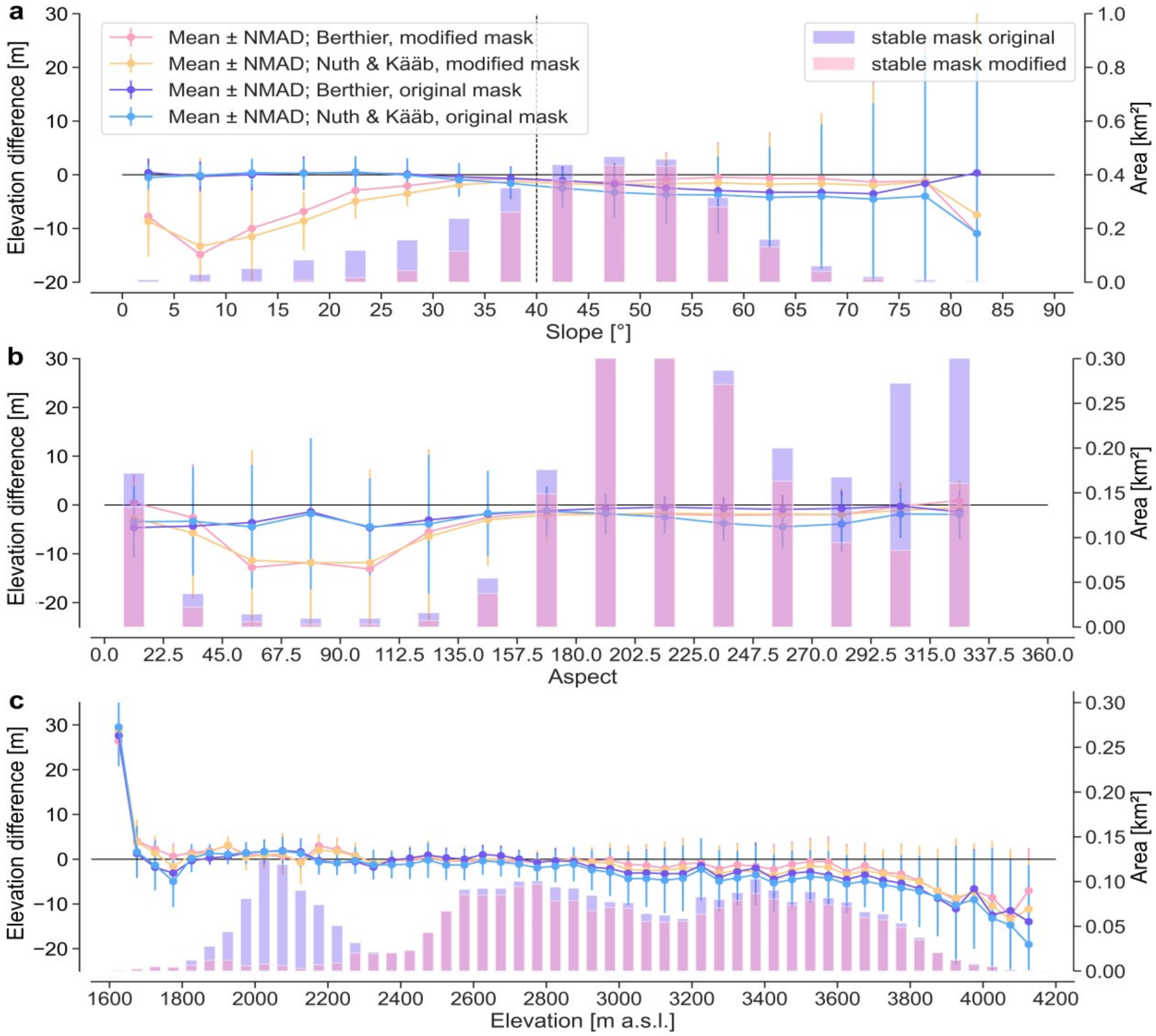

Fig. S8. Elevation differences over stable terrain with respect to slope (a), aspect (b), and elevation (c). Analog to **Fig. S3** but showing results for co-registration intercomparison. Area distributions for stable terrain (**Fig. S2**) and modified stable terrain (**Fig. S5**) are given on the second y-axis. Elevation differences are calculated from TanDEM-X minus Pléiades DEMs. Slope, aspect, and elevations are derived from the Pléiades DEM. Results are shown for common elevation bins. Note the very limited coverage of the modified stable terrain mask in many elevation bins.

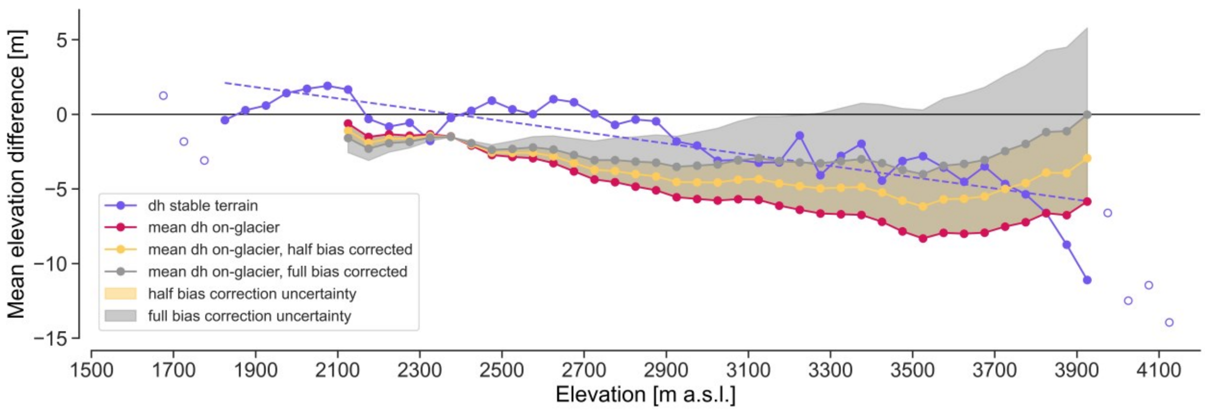

Fig. S9. Impact of potential corrections of elevation-dependent bias on elevation differences over the glacier. The correction is derived from the linear regression through mean elevation differences over stable terrain, excluding elevation bins with areas of ≤ 0.01 km^2 (indicated by open circles). The related bias corrections are estimated as half and full of the bias and applied to the dh over the glacier. The related uncertainty is estimated as ± one bias correction.